REPRODUCTION
RESEARCH

Clathrin is essential for meiotic spindle function in oocytes

Jurriaan J Hölzenspies[1,2], Bernard A J Roelen[1], Ben Colenbrander[1], Roland A P Romijn[3], Wieger Hemrika[3], Willem Stoorvogel[2] and Theo van Haeften[2]

Departments of [1]Farm Animal Health and [2]Biochemistry and Cell Biology, Faculty of Veterinary Medicine, Utrecht University, 3584 CM Utrecht, The Netherlands and [3]U-Protein Express BV, 3584 CH Utrecht, The Netherlands

Correspondence should be addressed to T van Haeften; Email: t.vanhaeften@uu.nl

Abstract

In the mammalian ovary, oocytes are arrested at prophase of meiosis I until a hormonal stimulus triggers resumption of meiosis. During the subsequent meiotic maturation process, which includes completion of the first meiotic division and formation of the second metaphase spindle, oocytes acquire competence for fertilization. Recently, it was shown that clathrin, a cytosolic protein complex originally defined for its role in intracellular membrane traffic, is also involved in the stabilization of kinetochore fibers in mitotic spindles of dividing somatic cells. However, whether clathrin has a similar function in meiotic spindles in oocytes has not been investigated previously. Our results show that endogenous clathrin associates with the meiotic spindles in oocytes. To study the function of clathrin during meiotic maturation, we microinjected green fluorescent protein-tagged C-terminal and N-terminal dominant-negative clathrin protein constructs into isolated porcine oocytes prior to *in vitro* maturation. Both protein constructs associated with meiotic spindles similar to endogenous clathrin, but induced misalignment and clumping of chromosomes, occurrence of cytoplasmic chromatin and failure of polar body extrusion. These data demonstrate that clathrin plays a crucial role in meiotic spindle function in maturing oocytes, possibly through spindle stabilization.

Reproduction (2010) **140** 223–233

Introduction

During development, mammalian oocytes are arrested at prophase I, and resume meiosis when maturation is initiated in response to the luteinizing hormone surge. Oocyte maturation is characterized by several key events, including disintegration of the nuclear envelope, also referred to as germinal vesicle breakdown (GVBD), formation of the first metaphase spindle, extrusion of the first polar body, and formation of the second metaphase spindle. In most mammals, oocytes enter a second period of meiotic arrest at metaphase II (MII), which is maintained until fertilization (Mehlmann 2005*b*, Richard 2007). Nondisjunction of chromosomes during the meiotic divisions of oocytes is a major source of genetic disorders in humans (Martin 2008), and it is thus important to understand the machinery that controls proper chromosome segregation. In mitotic cells, the kinetochore fibers of the metaphase spindle are associated with and stabilized by a large cytosolic protein, clathrin (Royle *et al*. 2005, Royle & Lagnado 2006).

Clathrin is a ubiquitously expressed protein, and has a prominent role in intracellular membrane transport pathways that rely on clathrin-coated vesicles (Kirchhausen 2000, Okamoto *et al*. 2000, Royle *et al*. 2005, Ungewickell & Hinrichsen 2007). Clathrin forms a large three-legged hexameric protein complex called triskelion, which is composed of three heterodimers of a ~190 kDa heavy chain (CHC) and a ~25 kDa light chain (CLC). Triskelions can polymerize into a polyhedral coat that drives the formation of clathrin-coated vesicles, which bud off from several membranes, including the plasma membrane and the trans-Golgi network (Kirchhausen 2000, Ungewickell & Hinrichsen 2007). A less well-known function of clathrin, independently of its role in membrane transport, is to prevent misalignment and mis-segregation of chromosomes in mitotic cells, presumably by bridging microtubules (Royle *et al*. 2005, Royle & Lagnado 2006). Clathrin-depleted somatic cells show diverse mitotic defects, including the activation of the spindle checkpoint and disruption of cytokinesis, culminating in aberrant chromosome segregation and incomplete cell division. Although clathrin has also been observed to associate with the second meiotic spindle in mouse oocytes (Maro *et al*. 1985), a role for clathrin in spindle function in maturing oocytes has not been established. Mammalian oocytes form spindles that are generally much larger than mitotic spindles, and arrest at MII after *in vitro* maturation, thus providing ideal conditions to study the spindle function of clathrin.

In the present study, we have investigated the role of clathrin in the meiotic progression of maturing porcine oocytes. Clathrin function at metaphase spindles

ISSN 1470–1626 (paper) 1741–7899 (online)
DOI: 10.1530/REP-10-0045
Online version via www.reproduction-online.org

requires both the N- and C-terminal domains of CHC in somatic cells (Royle *et al.* 2005, Royle & Lagnado 2006, Yamauchi *et al.* 2008). To interfere with clathrin function, we microinjected green fluorescent protein (GFP)-tagged constructs that constituted either the N- or the C-terminal domain of porcine CHC. Our data provide the first insight into the involvement of clathrin in mammalian oocyte maturation and demonstrate that clathrin is essential for meiotic spindle function.

Results

Distribution of endogenous clathrin during oocyte maturation

To investigate the distribution of endogenous clathrin, porcine oocytes were fixed either directly after isolation or after 44 h of *in vitro* maturation, immunolabeled for heavy chain clathrin and analysed using confocal laser scanning microscopy. All freshly isolated oocytes were at the GV stage, whereas nearly all 44 h matured oocytes reached the MII stage. In both immature GV and MII stage oocytes, CHC was distributed throughout the cytoplasm, but predominantly in association with punctate structures at the oocyte cortex, possibly corresponding to clathrin-coated vesicles (Fig. 1A and C). In MII stage oocytes, CHC was also observed at the metaphase spindle and in the polar body (Fig. 1C). Oocytes labeled for CLC showed similar patterns for both stages (data not shown). Control oocytes labeled with identical concentrations of negative control mouse IgG showed no staining at identical confocal settings (Fig. 1B and D), demonstrating the specificity of clathrin labeling. Notably, staining for CHC was relatively low in the surrounding cumulus cells, both at the onset of maturation and at MII arrest (Fig. 1A and C). The presence of clathrin on microtubules at the meiotic spindle was confirmed by immuno-double labeling 44 h matured oocytes for CHC and tubulin (Fig. 1E–H). To confirm that CHC associated with spindle fibers, 43 h matured oocytes were exposed to 10 μM nocodazole for 1 h to depolymerize the microtubules

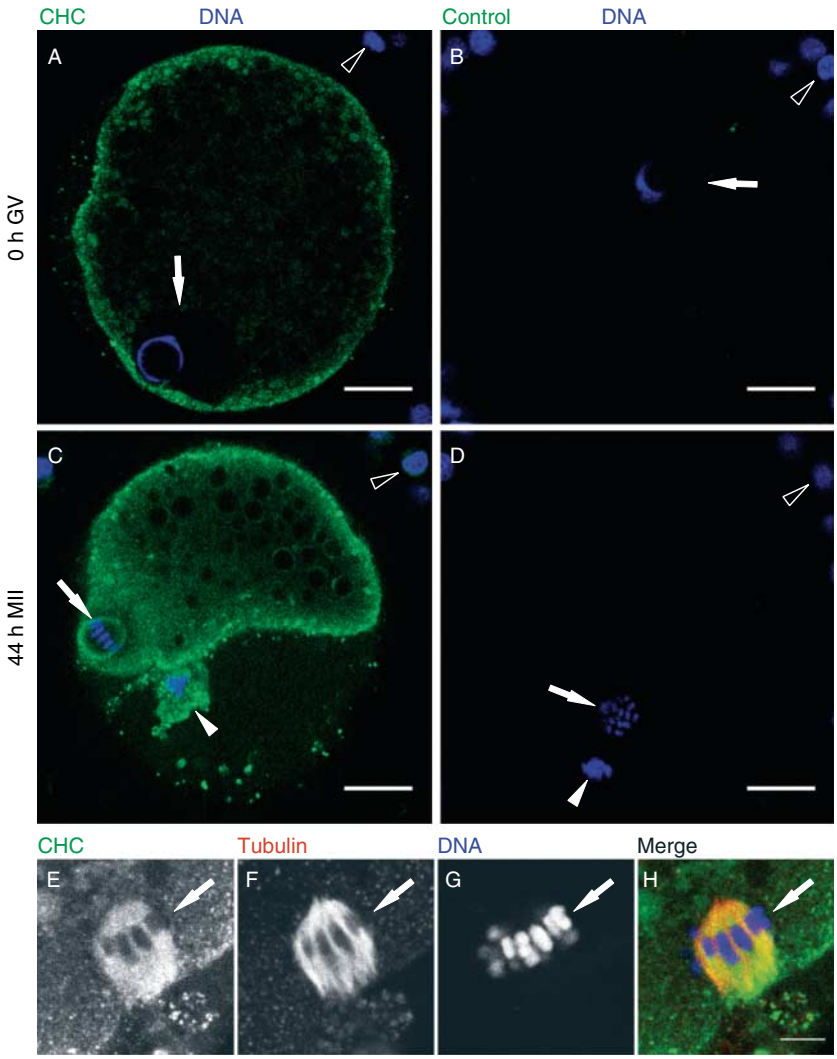

Figure 1 Distribution of endogenous clathrin during oocyte maturation. (A and B) 0 h GV stage oocytes labeled for DNA (blue) and CHC (A; green), or irrelevant control antibody (B; green). Arrows indicate the GV. (C and D) 44 h MII stage oocytes labeled for DNA (blue) and CHC (C; green), or irrelevant control antibody (D; green). Arrows and arrowheads indicate the MII spindle and the polar body respectively. Open arrowheads indicate cumulus cells that remained associated with the zona pellucida (not stained) in all images. Please note that the clathrin-stained oocytes in this figure show mild (GV stage) to severe (MII stage) denting of the plasma membrane, and this difference in fixation effects is presumably caused by the loss of gap junctions between the oocyte and the transzonal projections from the cumulus cells. The resulting morphology may appear to be aberrant, but is in fact normal for oocytes at these stages. Scale bars, 20 μm. (E–H) Single confocal section at an MII spindle of a 44 h matured oocyte labeled for CHC (E and green in H), tubulin (F and red in H), and DNA (G and blue in H), showing colocalization (yellow) of CHC and tubulin in the merge (H). Arrows indicate the metaphase plate. Scale bar, 10 μm.

that make up the spindle. Nocodazole-treated oocytes lacked both tubulin and clathrin labeling around the DNA in oocytes that showed an extruded polar body, whereas these labels were present around the DNA in DMSO-treated controls and nocodazole-treated oocytes that were allowed to recover for 1 h (Supplementary Figure 1, see section on supplementary data given at the end of this article). Collectively, these data demonstrate that the association of clathrin with the spindle relies on the presence of intact microtubules.

Clathrin constructs

To study clathrin function during oocyte maturation, truncated dominant-negative GFP-tagged CHC protein constructs were first generated using transfected HEK293E cells and isolated to homogeneity (see Materials and Methods section and Fig. 2A). The C-terminal construct (GFP-C-CHC) contained the CHC trimerization domain, the CLC-binding domain, and GFP- and His-tags at its N-terminus. A similar construct was previously shown to trimerize with endogenous clathrin and inhibit clathrin-mediated endocytosis in HeLa cells (Liu *et al.* 1998). Since trimerization of clathrin is also important for its function on spindles in somatic cells (Royle & Lagnado 2006), GFP-C-CHC was expected to interfere with the spindle function of clathrin in oocytes. The N-terminal construct (N-CHC-GFP) encompassed a domain that was previously demonstrated to interfere with clathrin-mediated endocytosis and to associate with mitotic spindles in somatic cells (Royle *et al.* 2005), and contained GFP- and His-tags at its C-terminus. We also tried to produce these dominant-negative CHC protein constructs with GFP-tags on the other side and a GFP-tagged full-length CHC construct. Unfortunately, these constructs were not stably expressed by our producer cell line. Instead, non-conjugated GFP was used as a negative control.

Isolated constructs were then microinjected into immature oocytes. To control for the amount of injected protein, total GFP fluorescence in oocytes was measured by epifluorescence microscopy (Lee 1989) directly after injection (Fig. 2B). Of successfully injected oocytes, total fluorescence did not differ significantly between oocytes injected with GFP or either one of the CHC constructs (Fig. 2C). After injection, oocytes were allowed to mature for 44 h, fixed, immunolabeled for tubulin, and stained for DNA. Consistent with the distribution of endogenous clathrin, both N-CHC-GFP and GFP-C-CHC accumulated at the meiotic spindle (Fig. 3A and B). To quantify recruitment of CHC constructs to the meiotic spindles (Royle *et al.* 2005), we determined GFP fluorescence intensities in representative areas on the spindle relative to the oocyte cortex (Fig. 3A–C). Both N-CHC-GFP and GFP-C-CHC were significantly enriched on the spindle in comparison with non-conjugated GFP (Fig. 3D).

Clathrin constructs disrupt meiotic divisions in oocytes

Our next step was to investigate the effects of injected N-CHC-GFP and GFP-C-CHC on oocyte maturation. A normal MII pattern was observed in the majority of oocytes that were injected with non-conjugated GFP

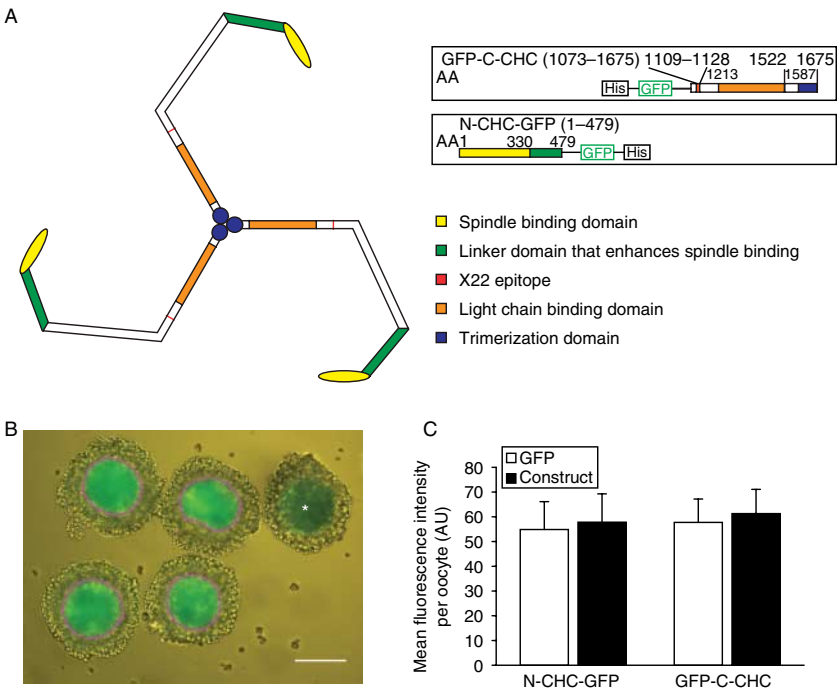

Figure 2 Clathrin constructs. (A) Schematic overview of the CHC constructs. The color-coded domains on the constructs are indicated in identical colors on the clathrin triskelion shown on the left, and the location of the GFP tag on each of the constructs is shown on the right. (B) Merged brightfield and fluorescent images showing five oocytes injected with GFP-C-CHC. As an example, the oocyte marked with * was removed from the experiment immediately after injection based on its relatively low fluorescence intensity. A region of interest (ROI; shown in magenta) was drawn around the remaining four oocytes by thresholding the fluorescent image (the same threshold was used for all injection experiments in this study). (C) Bar graph showing measured total fluorescence within threshold-generated ROIs for injected oocytes. Bars represent mean fluorescence intensity ±S.D. in arbitrary units (AU) of 45–63 oocytes from three independent experiments. For the experiments in Figs 3–6, no significant difference in fluorescence intensity was found between oocytes injected with N-CHC-GFP ($P=0.24$), GFP-C-CHC ($P=0.09$), or GFP using a two-tailed homoscedastic Student's *t*-test.

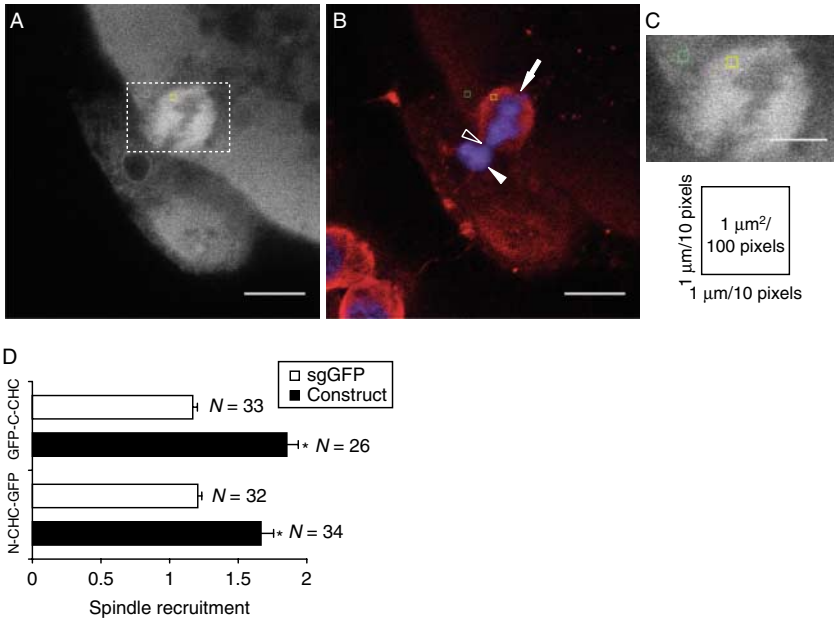

Figure 3 Clathrin constructs specifically localize to the meiotic spindle. (A) An oocyte showing the distribution of injected N-CHC-GFP. (B) The distributions of tubulin (red) and DNA (blue) in the same oocyte as in A, showing a typical phenotype observed in CHC construct-injected oocytes, which is characterized by clumping of the chromatin on the MII spindle (arrow) and an extruded polar body (arrowhead) that remained attached to the spindle via a 'DNA bridge' (open arrowhead). Scale bars, 20 µm. (C) Enlargement of the area indicated by the dashed rectangle in A. Scale bar, 5 µm. A schematic representation indicating the size of the regions of interest (ROIs) on the spindle (yellow square) and in the cortex (green square) is shown below the image. Spindle recruitment was calculated by dividing the mean GFP fluorescence intensity in the ROI on the spindle by that in the cortex. To calculate spindle recruitment, two ROIs on the spindle (one on each side of the metaphase plate) and two ROIs in the cortex were analysed for each oocyte. To ensure objective measurements, each spindle/cortex-pair of ROIs was created within a single confocal section showing only tubulin and DNA staining (as in B) and transposed onto the equivalent section showing GFP fluorescence (as in A). (D) Bar chart showing spindle recruitment in oocytes injected with control GFP or CHC constructs. Bars represent mean spindle recruitment ±S.E.M. from three independent experiments, and the number of oocytes analysed (N) is shown next to each bar. Both N-CHC-GFP ($P<0.001$) and GFP-C-CHC ($P<0.001$) revealed significantly higher recruitment to MII spindles (asterisks) compared with GFP in injected oocytes using a two-tailed heteroscedastic Student's *t*-test.

(Figs 4A–D and 5A and B). Severe defects were observed, however, in both N-CHC-GFP- and GFP-C-CHC-injected oocytes. Both CHC constructs caused misalignment of chromosomes on the metaphase plate and formation of large clumps of condensed chromatin interspersed with patches of less condensed chromatin (Fig. 4E–T). In addition, chromosomes were regularly observed outside the metaphase spindle (e.g. open arrowhead in Fig. 4Q–T), and the polar body often remained connected to the oocyte via a 'DNA bridge' (open arrowheads in Fig. 4E–P) that varied in thickness and length between the injected oocytes (short and thin in Fig. 4E–H, short and thick in Fig. 4I–L, and long and thin in Fig. 4M–P). These bridges displayed no tubulin labeling, indicating that the spindle midbody was no longer present. These phenotypes are illustrated more clearly in Supplementary Movies 1–4 (see section on supplementary data given at the end of this article) which show 360° rotations of 3D reconstructions of the same oocytes as in Fig. 4A–H. In a subset of GFP-C-CHC-injected oocytes, condensed chromosomes were scattered throughout the area around the metaphase spindle. These scattered chromosomes formed small clusters that also contained tubulin (open arrowheads in Fig. 4Q–T) creating small spindle-like structures. Since defects at MII may result from abnormal progression through meiosis I (MI), oocytes that were arrested at MI after 44 h of maturation were also examined in detail. Typical aberrant MI morphology observed in these construct-injected oocytes included incomplete condensation and clumping of chromosomes (Fig. 6), abnormally dense astral microtubule networks (Fig. 6E–H), loose chromosomes outside the metaphase plate (filled arrowheads in Fig. 6), and tubulin fibers that connected the spindle to the loose chromosomes (open arrowheads in Fig. 6I–P).

To quantify the effects of the CHC constructs on oocyte maturation, 44 h matured oocytes were scored into four categories based on their tubulin and DNA staining patterns: aberrant GV (clearly visible nucleus), aberrant MI (with oocytes from prometaphase I up to and including telophase I), aberrant MII (clearly visible metaphase spindle and polar body, showing abnormal structure), and normal MII (clearly visible metaphase spindle and polar body). Oocytes that showed a normal GV or MI pattern after maturation were also scored as aberrant, since these oocytes failed to complete

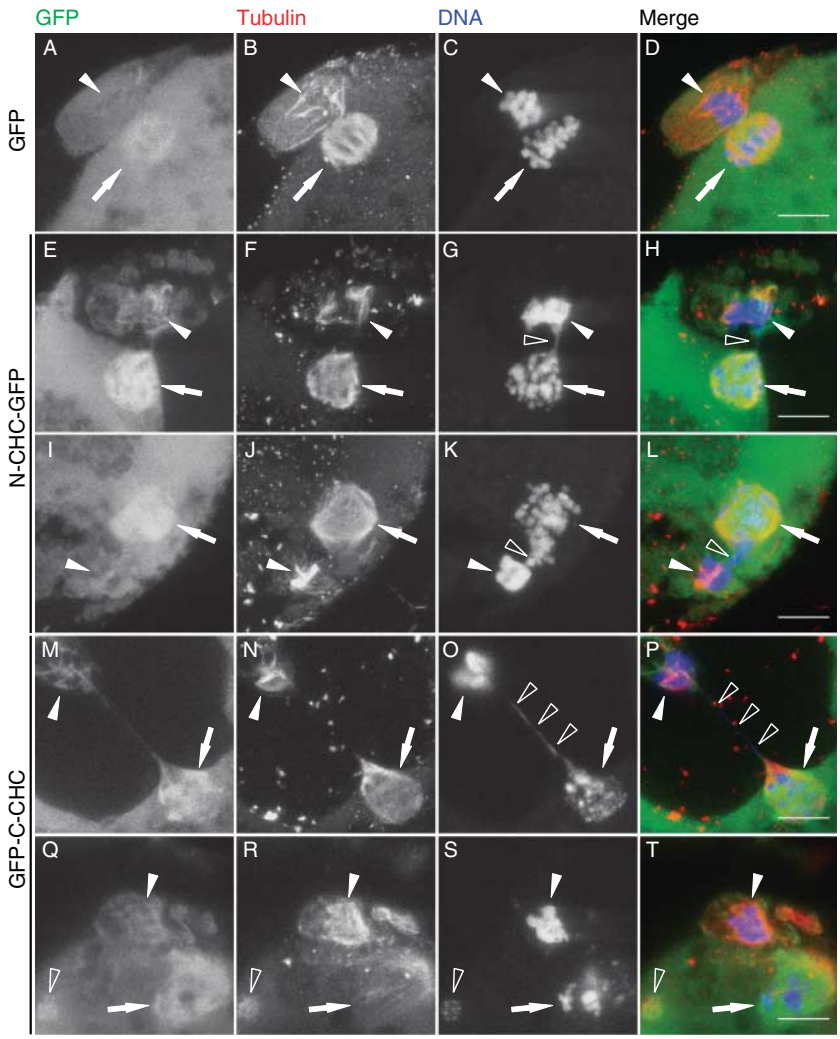

Figure 4 Aberrant MII profiles generated in response to clathrin constructs. Oocytes were injected with GFP or GFP-CHC constructs (left column and green in the merged fourth column), matured for 44 h, fixed, and labeled for the presence of tubulin (second column and red in the merged fourth column) and DNA (third column and blue in the merged fourth column). (A–D) Control GFP-injected oocyte showing a normal MII spindle and polar body. (E–L) Two examples of N-CHC-GFP-injected oocytes showing patchy condensation of chromosomes on the MII spindle and a 'DNA bridge' (open arrowheads) between the spindle and the polar body. (M–T) Two examples of GFP-C-CHC-injected oocytes showing either a long DNA bridge (open arrowheads in M–P), or misaligned chromosomes on the metaphase spindle (arrow in Q–T) and cytoplasmic chromatin (open arrowheads in Q–T). Filled arrows and arrowheads indicate the position of the MII spindle and polar body respectively. Scale bars, 10 μm.

maturation. Oocytes that could not be scored into any of these categories (~4%) were excluded from the analysis. Of the non-injected and GFP-injected oocytes, 60–70% showed normal morphology at MII (Fig. 5A and B). In contrast, of the N-CHC-GFP- and GFP-C-CHC-injected oocytes, only 13 and 2% respectively reached normal MII, while most showed an aberrant MII morphology. Statistical analysis of these data shows that oocytes injected with N-CHC-GFP or GFP-C-CHC were significantly inhibited in progressing through maturation as compared with GFP-injected oocytes. In both N-CHC-GFP and GFP-C-CHC conditions, the strongest significant effect was found for the ratio of aberrant versus normal MII oocytes compared with that in the control group. The ratio of aberrant MI versus normal MII oocytes was, however, also significantly higher for both CHC constructs. Only GFP-C-CHC-injected oocytes differed significantly in comparison with the control group in the ratio of aberrant GV versus normal MII phenotypes. A summary of these results and their significance is shown in Fig. 5C.

To specify MII aberrancies in more detail, we scored aberrant MII oocytes by phenotype using the following categories: misaligned chromosomes (chromatin outside the equator of the MII spindle), chromosome clumps (large clumps of condensed chromatin interspersed with patches of less condensed chromatin), DNA bridge (direct link between chromatin in the polar body and the oocyte) and cytoplasmic chromatin (loose chromosomes present in the cytoplasm). Almost all oocytes injected with either one of the CHC constructs showed misaligned chromosomes and chromosome clumps, whereas DNA bridges and cytoplasmic chromatin were observed in only 20–45% of oocytes. Statistical analysis of these results using χ^2 tests did not reveal any significant differences between N-CHC-GFP- and GFP-C-CHC-injected oocytes, suggesting that the effects of these constructs on oocyte maturation were identical (Fig. 5D).

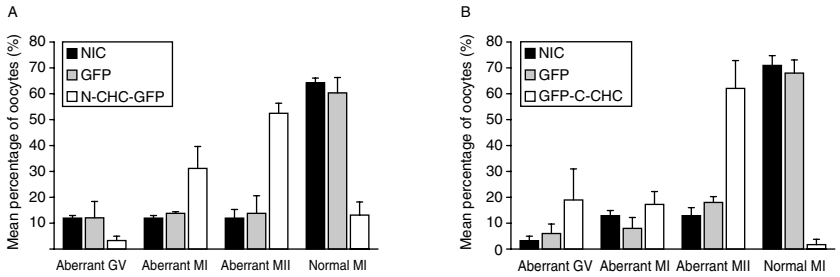

C

	Aberrant GV % OR (95% CI)	Aberrant MI % OR (95% CI)	Aberrant MII % OR (95% CI)	Normal MII % REF	*N*
NIC	7.75% 0.79 (0.31–2.01)	12.40% 1.06 (0.47–2.38)	12.40% 0.75 (0.35–1.58)	67.44% REF	6
GFP#	9.26% NA	10.19% NA	15.74% NA	64.81% REF	6
N-CHC-GFP	3.28% 1.72 (0.32–9.31)	31.15% 13.66** (4.88–38.20)	52.46% 16.24** (6.35–41.53)	13.11% REF	3
GFP-C-CHC	18.97% 75.90** (8.82–652.83)	17.24% 57.50** (6.73–491.23)	62.07% 146.10** (18.68–1142.41)	1.72% REF	3

OR = odds ratio
95% CI = 95% confidence interval
REF = reference stage
NA = not applicable
N = number of experiments
= control used for comparison
**P* < 0.05; ** *P* < 0.01

D

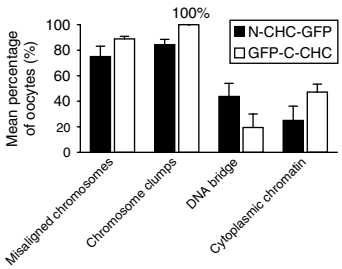

Figure 5 Quantification of aberrant meiotic profiles after injection of clathrin constructs. (A and B) Bar graphs showing percentages of 44 h matured oocytes at various stages after injection as determined in Fig. 4. Bars represent weighted mean percentage±weighted S.E.M. ($N=3$ independent experiments) of oocytes at the indicated stages. The indicated conditions are non-injected control oocytes (NIC; 67 and 62 oocytes in A and B respectively), GFP-injected oocytes (GFP; 58 and 50 oocytes in A and B respectively), N-CHC-GFP-injected oocytes (N-CHC-GFP; A; 61 oocytes), and GFP-C-CHC-injected oocytes (GFP-C-CHC; B; 58 oocytes). Significance of the results is indicated in the results section. (C) Table showing a summary of the analysis of the data shown in (A) and (B). The ratio of oocytes at each aberrant stage versus oocytes at the reference stage (normal MII) was compared between NIC/N-CHC-GFP/GFP-C-CHC and GFP conditions using multinomial logistic regression models. Several models were employed to investigate the interaction between maturation stage, which was used as an ordinal variable, and condition. Based on a minimized Akaike information criterion (AIC) value, a model that incorporated both N-CHC-GFP and GFP-C-CHC conditions and their respective controls, and used experiment number to control for random effects was chosen for final analysis. Significance of the results is indicated by asterisks ($P<0.01$). (D) Aberrant MII oocytes in (A) and (B) were scored for observed defects and analysed by χ^2 tests, which did not reveal any significant differences between N-CHC-GFP- and GFP-C-CHC-injected oocytes ($P>0.05$; Bonferroni corrected).

Discussion

In this study, we have demonstrated that clathrin is associated with meiotic spindles in porcine oocytes, and that interference with clathrin function by injection of dominant-negative CHC protein constructs disrupted meiosis progression. Moreover, our results support the notion that clathrin is involved in chromosome segregation during oocyte meiosis.

Clathrin is a cytosolic protein that, in addition to its role in membrane transport, was recently shown to stabilize the mitotic spindle in somatic cells (Royle *et al.* 2005, Royle & Lagnado 2006). This role for clathrin in mitosis was later questioned for a chicken pre-B lymphoma cell line (DKO-R). Although the localization of clathrin at the spindle during mitosis is highly consistent between different cell lines, clathrin-depleted DKO-R cells did not show mitotic defects (Royle *et al.* 2005, Borlido *et al.* 2008). These data suggest the existence of cell type-specific differences in spindle-associated clathrin function. It should be noted, however, that DKO-R cells were specifically developed to study clathrin function while preventing apoptosis caused by clathrin depletion, and could have acquired adaptations that attenuate the mitotic phenotype of clathrin depletion that was observed in other cell lines (Wettey *et al.* 2002, Royle *et al.* 2005, Borlido *et al.* 2008). Although the necessity of clathrin function on mitotic spindles may vary between different cell lines, a conserved role for clathrin in stabilizing meiotic spindles is plausible, given that spindle instability is closely linked to aneuploidy (Jones 2008). Although clathrin also serves as an important factor in intracellular membrane transport (Kirchhausen 2000, Ungewickell & Hinrichsen 2007), the potential functions of clathrin in oocytes have not been investigated previously. Consistent with previous observations for mouse MII oocytes (Maro *et al.* 1985), we demonstrate by immunofluorescence microscopy that clathrin associates with metaphase spindles in porcine oocytes (Fig. 1). The initial observations by Maro *et al.* (1985) were thought to reflect association of clathrin-coated vesicles with spindle fibers. In somatic cells, however, clathrin was shown to bind the mitotic spindle directly, while membranes did

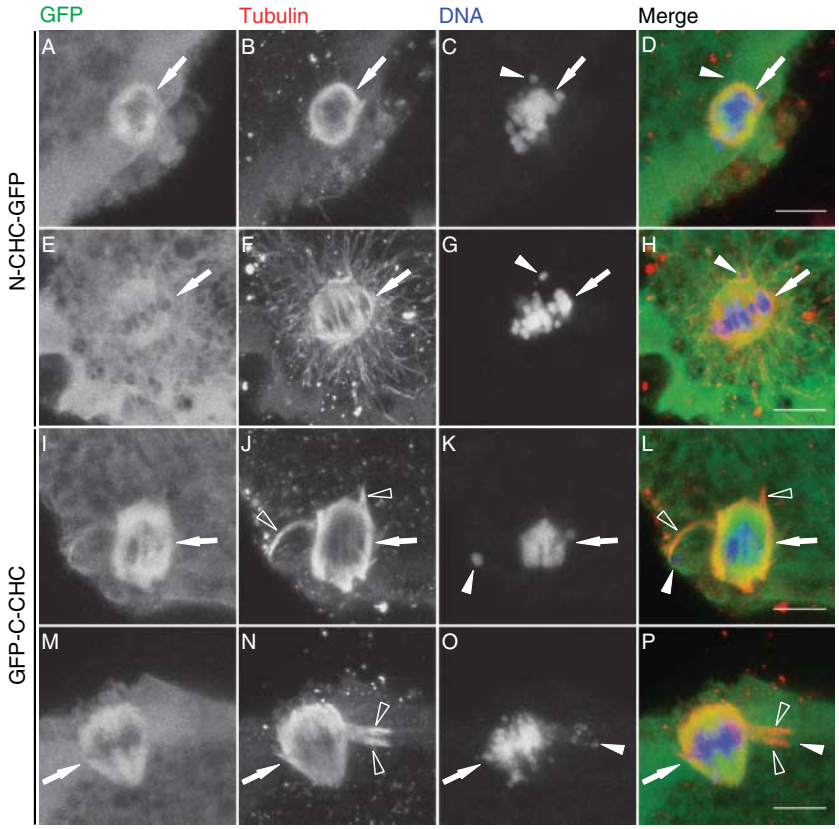

Figure 6 Aberrant MI profiles in response to clathrin constructs. Labeling and imaging of oocytes were performed as in Fig. 4. Examples of N-CHC-GFP-injected (A–H) and GFP-C-CHC-injected (I–P) oocytes arrested at MI after 44 h of maturation are shown. These MI arrested oocytes show clumping of chromosomes on the metaphase plate, abnormal spindle morphology and 'loose' chromosomes that have failed to align on the metaphase plate. Arrows indicate the metaphase plate, filled arrowheads indicate 'loose' chromosomes and open arrowheads indicate tubulin fibers that emanate from the spindle. Maximum intensity Z projections of three consecutive confocal sections (2 μm intervals) are shown. Scale bars, 10 μm.

not associate with the spindle (Royle *et al*. 2005, Royle & Lagnado 2006). Using lipophilic dyes, we could not detect association of membranes with the meiotic spindle in oocytes (data not shown). Moreover, clathrin did not persist at the spindle upon depolymerization of spindle microtubules using nocodazole, and was recovered together with spindle microtubules within 1 h of nocodazole removal (Supplementary Figure 1). These data suggest that clathrin does not associate with the spindle matrix, as nocodazole-mediated depolymerization of the spindle in mitotic cells was previously shown to leave the spindle matrix in place (Lince-Faria *et al*. 2009).

Unlike somatic cells, fully grown mammalian oocytes are characterized by repressed transcription (Motlik *et al*. 1984, Fair *et al*. 1996, Bouniol-Baly *et al*. 1999, De La Fuente & Eppig 2001, Bjerregaard & Maddox-Hyttel 2004), and oocytes thus cannot be manipulated by cDNA transfection. Given the ubiquitous and crucial functions of clathrin, clathrin knockout animals have not been generated, and conditional knockout systems for clathrin in oocytes are not available. RNAi knockdown of endogenous clathrin in oocytes is also extremely unlikely to succeed, because clathrin is one of the most abundant proteins in cells (Goud *et al*. 1985), and has a very long half-life (Acton & Brodsky 1990). Indeed, even in highly active mitotic cells, CHC RNAi does not show an effect on the mitotic index until 48 h after transfection (Royle *et al*. 2005). Although exogenous proteins can be expressed by injection of mRNA in porcine oocytes, the efficiency of such injection procedures is low (~30% of injected oocytes showed expression during maturation), and expression levels vary extensively between oocytes (Ohashi *et al*. 2001). Instead, the method used here to microinject dominant-negative clathrin protein constructs was highly efficient (~75% of injected oocytes showed sustained fluorescence), and allowed instantaneous introduction of a reproducible amount of exogenous protein into each oocyte (Fig. 2). These microinjected GFP-tagged constructs, corresponding to the N- or C-terminal domains of CHC (Fig. 2), were both recruited to MII spindles (Fig. 3). N-CHC-GFP, which contains the previously determined spindle-binding domain (Royle *et al*. 2005), was recruited to the meiotic spindle to the same extent as GFP-C-CHC (Fig. 3). These observations suggest that both constructs contain spindle recruitment domains, although it cannot be excluded that our constructs have been recruited to the spindle by associated endogenous full-length CHC that may have been incorporated in 'mixed' triskelions. A recent study showed that formation of a complex, which consists of clathrin, B-Myb, and filamin, is required for recruitment of clathrin to the mitotic spindle in somatic cells, and the authors suggested that the C-terminal trimerization

domain of clathrin could also be involved in the formation of this complex (Yamauchi *et al*. 2008). In another study, the N-terminal domain appeared to be indispensable for spindle localization, since a construct lacking this domain (331–1639) failed to be recruited to mitotic spindles (Royle & Lagnado 2006). It should be noted that these results were obtained in somatic cells that had been depleted of endogenous clathrin by RNAi, and as such did not allow formation of mixed triskelions containing both endogenous CHC and the truncated CHC construct.

Oocytes injected with either one of our CHC constructs displayed severe defects in MII morphology (Figs 4 and 5) while maturation rates and MII morphology of GFP-injected control oocytes did not differ from those of non-injected controls (Figs 4A–D and 5A and B). Both CHC constructs caused misalignment of chromosomes and formation of chromosome clumps, which may be explained by CHC construct-induced failure of the spindle checkpoint during MI. When some homologous chromosomes separate normally and others remain attached to each other and are pulled either into the nascent polar body or into the oocyte, chromosome clumps would form on the second metaphase spindle. Moreover, the aberrant presence of homologous chromosome pairs on the second metaphase spindle may disrupt proper chromosome alignment. Indeed, oocytes that were arrested at MI after 44 h of maturation as a consequence of the injection of CHC constructs showed congression failure (Fig. 6). In spite of this severe phenotype observed in some of the injected oocytes, the majority of oocytes that were injected with the CHC constructs did not arrest at MI (Fig. 5A and B), indicating failure of the MI spindle checkpoint. Although these inferences remain speculative, it is clear that future research on clathrin function in meiotic spindles should include investigation of checkpoint controls, particularly since clathrin adaptor proteins have been implicated in spindle function and checkpoint control in mitotic cells (Cayrol *et al*. 2002, Lehtonen *et al*. 2008).

Clathrin-mediated endocytosis may also have been affected by our CHC constructs. A possible effect of interference with endocytosis is failure of polar body cytokinesis, since it has been demonstrated that endocytosis at the cleavage furrow is important for cytokinesis in several types of mitotic cells (Niswonger & O'Halloran 1997, Feng *et al*. 2002, Schweitzer *et al*. 2005, Albertson *et al*. 2005, Warner *et al*. 2006, Montagnac *et al*. 2008). These findings suggest that endocytosis may also be important for cytokinesis in oocytes. We observed that respectively 44 and 19% of N-CHC-GFP- or GFP-C-CHC-injected oocytes remained connected to their polar body via a DNA bridge (Figs 4E–P and 5D), demonstrating that chromosome segregation is incomplete in these oocytes. These cytoplasmic connections between oocytes and their polar bodies did not contain tubulin, suggesting that the spindle midbody, which may be involved in abscission during cytokinesis (Montagnac & Chavrier 2008), was no longer present. These results are indicative of destabilization of the first meiotic spindle, given that cytokinesis is normally preceded by chromosome segregation. We conclude that interference with endocytosis-dependent cytokinesis cannot explain our results. Studies on *Xenopus* oocytes demonstrated that meiosis resumption involves endocytosis of a G-protein-coupled receptor (Wang & Liu 2003, El-Jouni *et al*. 2007). The G-protein-coupled receptor GPR3 appears to be required for maintenance of meiotic arrest in mouse, rat, and human oocytes (Mehlmann *et al*. 2004, Hinckley *et al*. 2005, Mehlmann 2005*a*, DiLuigi *et al*. 2008), suggesting that endocytosis of this receptor may also be involved in resumption of oocyte meiosis in mammals. Since clathrin is required for endocytosis of specific receptors in somatic cells (Kirchhausen 2000, Moore *et al*. 2007, Ungewickell & Hinrichsen 2007), these findings suggest an alternative role for clathrin in resumption of meiosis. Constructs similar to our CHC constructs have been demonstrated to interfere with membrane traffic in somatic cells (Liu *et al*. 1998, Royle *et al*. 2005). In our study, however, meiosis progression beyond GVBD was not affected in the majority of CHC construct-injected oocytes (Fig. 5A and B). Therefore, inhibition of G-protein-coupled receptor endocytosis cannot explain our results.

Taken together, our findings in porcine oocytes are consistent with a role for clathrin in stabilizing metaphase spindles (Royle *et al*. 2005, Royle & Lagnado 2006). Disruption of clathrin function in maturing oocytes causes severe spindle-related defects, which may be due to spindle checkpoint failure and/or spindle destabilization during MI. Although we have established that clathrin plays a pivotal role in meiosis progression during porcine oocyte maturation, further research will be required to untangle the contributions of its functions to meiotic spindle stability.

Materials and Methods

Recombinant clathrin constructs

Porcine clathrin heavy chain was PCR amplified from porcine brain cDNA using the Expand Long Template PCR System (ELT-PCR; Roche Applied Science, Indianapolis, IN, USA) according to the manufacturer's instructions with primers designed based on homology between the known human (NM_004859), bovine (NM_174023), and mouse (NM_001003908) CHC sequences (Table 1, Primers for PCR), and sequenced (Baseclear, Leiden, The Netherlands; EMBL accession number FM210346, accession date 3 March 2009). The PCR product was then diluted 1:1000 and amplified again using Pfu DNA polymerase (Fermentas, Burlington, Ontario, Canada) to obtain coding cDNA for residues 1–479 (N-CHC) and residues 1073–1675 (C-CHC) and to introduce in-frame BamHI – NotI restriction sites for C-terminal clathrin and

Table 1 Primers for full-length, C-terminal and N-terminal clathrin heavy chain.

Primers for PCR	**Forward**	**Reverse**
Full-length clathrin + UTRs	5′-GGA GGA GAC CAT ACC CCC CGA CAG-3′	5′-AAC AGA TTG AAT ATT AAG CAG T-3′
Cloning primers	**BsaI site** (5′-GGTCTC(N)$_6$-3′) **BamHI site** (5′-GGATCC-3′)	**NotI** site (5′-GCGGCCGC-3′)
Full-length clathrin	5′-GGG GTC TCG GAT CCG CCC AGA TTC TGC CAA TTC GTT TTC AGG-3′	5′-GCG GCC GCC ATG CTG TAC CCA AAG CCA GGC TG-3′
C-terminal clathrin	5′-GGA TCC AAA TTT GAT GTC AAT ACT TCA GCA GTG CAG GTC-3′	5′-GCG GCC GCC ATG CTG TAC CCA AAG CCA GGC TG-3′
N-terminal clathrin	5′-GGG GTC TCG GAT CCG CCC AGA TTC TGC CAA TTC GTT TTC AGG-3′	5′-GCG GCC GCG TAT ACA CTA AGT GCC AAT GTC GGG TCC-3′

BsaI – NotI for N-terminal clathrin (Table 1, cloning primers). Both constructs were cloned into pCR4-TOPO (Invitrogen, Paisley, UK), and positive clones were sequenced (Baseclear). N- and C-terminal CHC constructs were then ligated into pUPE (U-Protein Express BV, Utrecht, The Netherlands) containing the Superglo GFP sequence followed by a His-tag at the N-terminus of the C-terminal construct and at the C-terminus of the N-terminal construct. Recombinant CHC constructs were expressed in HEK293E cells. HEK293E cells from a 1-l suspension culture were pelleted by centrifugation and resuspended in 0.5 M Tris–HCl, pH 7.5 containing protease inhibitor (Roche), lysed by repeated freeze–thawing and further homogenized in a Potter–Elvehjem homogenizer. Nuclei, organelles, and large protein complexes were removed by sequential centrifugation steps at 1000 ***g*** for 20 min, 20 000 ***g*** for 20 min, and finally 200 000 ***g*** for 1.5 h. Protein constructs were purified from the resulting supernatant by Ni^{2+}-affinity chromatography (Ni Sepharose FF, GE Healthcare Europe GmbH, Diegem, Belgium). Efficient elution from the Ni Sepharose column was achieved using 25 mM Tris–HCl (pH 8.5), 500 mM NaCl, 500 mM imidazole for C-terminal, and 25 mM Tris–HCl (pH 7.5), 100 mM EDTA for N-terminal clathrin protein constructs. Eluted proteins were subsequently subjected to gel filtration (Superdex 200 pg 16/600; GE Healthcare) and concentrated in microinjection buffer (120 mM KCl, 20 mM HEPES–KOH, pH 6.9; adjusted from Amano *et al.* (2004)) using Vivaspin tubes with a 10-kDa molecular weight cut-off (GE Healthcare). The yields of N- and C-terminal CHC constructs were ∼1 mg/ml protein in 2 and 0.8 ml of microinjection buffer respectively. GFP (Superglo GFP; Qbiogene, Montreal, Quebec, Canada) was dialyzed in the same microinjection buffer and used as negative control. Supplementary Figure 2 (see section on supplementary data given at the end of this article) shows control GFP and purified N- and C-terminal clathrin protein constructs separated by SDS-PAGE on a 10% polyacrylamide gel stained with coomassie.

Oocyte isolation, selection, microinjection and culture

All chemicals were purchased from Sigma Chemical Co., unless otherwise indicated. Cumulus–oocyte complexes (COCs) were collected by aspiration from 3 to 6 mm follicles from sow (*Sus scrofa*) ovaries, which were acquired from a slaughterhouse. The collected COCs were allowed to settle and washed several times in a buffer containing 114 mM NaCl, 3.2 mM KCl, 2 mM $NaHCO_3$, 0.4 mM $NaH_2PO_4{\cdot}H_2O$, 0.25 mM sodium pyruvate, 10 mM sodium lactate, 0.5 mM $MgCl_2{\cdot}6H_2O$, 2 mM $CaCl_2{\cdot}2H_2O$, 10 mM HEPES, 0.1% (w/v) polyvinylpyrrolidone (PVP), 1 mM dibutyryl cAMP (dbcAMP), pH 7.4. Oocytes were maintained in prophase arrest during collection and microinjection by the presence of dbcAMP. Prior to injection, oocytes were partially denuded by gentle pipetting until 3–6 layers of cumulus remained, and washed in HEPES-buffered M199 from Gibco BRL (Grand Island, NY, USA) supplemented with 1 mM dbcAMP. For injection, groups of five oocytes were placed in 5 µl drops of this medium under oil at 37 °C on an IX71 inverted microscope (Olympus, Zoeterwoude, The Netherlands) equipped with a heated stage and an epifluorescence setup. A suction pipette was used to immobilize oocytes, and beveled rigid borosilicate micropipettes with a 30° angle and a 3.5 µm tip diameter (custom tips; Eppendorf, Hamburg, Germany) were used to perform injections. Injection solutions were centrifuged for 10 min at 16 000 ***g*** just prior to use, and ∼1 µl was backloaded into the micropipettes, which were subsequently connected to a Femtojet pressure injection system (Eppendorf). Immediately after injection, epifluorescent images were recorded on the IX71 microscope at 100× magnification through a FITC filter using a DP20 camera (Olympus) at 100 ms exposure. Any oocytes showing much higher or lower fluorescence intensity than average (typically 20–30% of injected oocytes) were immediately removed from the experiment (see for example Fig. 2B). To ensure that equal amounts had been injected between groups, the epifluorescence images taken during injection experiments were evaluated by measuring the total GFP fluorescence per oocyte in ImageJ. Total fluorescence was measured in regions of interest (ROIs) around injected oocytes. ROIs were generated using a fixed threshold, which was kept identical between experiments. *In vitro* maturation was performed as described previously (Hölzenspies *et al.* 2009).

Immunofluorescence and confocal microscopy

COCs were washed and denuded by gentle pipetting in 80 mM PIPES, 5 mM EGTA, 2 mM $MgCl_2$, 0.3% (w/v) PVP, pH 6.9 at 37 °C (PEM–PVP), and then fixed in PEM–PVP containing 4% (v/v) paraformaldehyde (Electron Microscopy Sciences, Hatfield, PA, USA) at room temperature for 1 h. After fixation, oocytes were washed twice in 0.1 M phosphate buffer (pH 7.4) containing 0.3% (w/v) PVP, and permeabilized in 0.1 M phosphate buffer supplemented with 0.1% (w/v) saponin (Riedel de Haen AG, Seelze, Germany). Permeabilized oocytes were blocked in 0.1 M phosphate buffer containing 0.1% (w/v)

saponin, 1% (w/v) BSA and 2% (v/v) normal goat serum (Vector Lab, Burlingame, CA, USA) supplemented with 100 mM glycine for 2 h at room temperature. After this blocking step, oocytes were subjected to sequential 1 h incubations with primary and secondary antibodies, which had been diluted in blocking solution without glycine and centrifuged at 100 000 ***g*** for 1 h before use. To label microtubules, a mixture of rabbit polyclonal antibodies directed against α-tubulin (1:400; Abcam, Cambridge, UK) and β-tubulin (1:400; Sigma) was used. Clathrin was labeled with CON.1, which is directed against a conserved region (AA 23–44) of CLC (Nathke *et al.* 1992), and X22, which is directed against a conserved region (AA 1109–1128) near the C-terminus of CHC (Brodsky 1985, Liu *et al.* 1995). CON.1 and X22 were produced from hybridoma cultures in our lab (kindly provided by Dr F M Brodsky). Irrelevant primary antibodies of the same isotype (Sigma) and at identical concentrations were used as negative controls. Secondary antibodies were goat anti-mouse IgG alexa488 and goat anti-rabbit IgG alexa568 (Molecular Probes, Eugene, OR, USA), and DNA was labeled for 20 min with 10 μM TO-PRO-3 iodide (Molecular Probes). Each labeling step was followed by three washes in 0.1 M phosphate buffer supplemented with 0.1% (w/v) saponin. Finally, oocytes were sealed in Vectashield (Vector Lab) on Superfrost Plus microscope slides (Menzel, Braunschweig, Germany) in 0.12 mm Secure-Seal Spacers (Molecular Probes).

Confocal images were obtained using a Nikon eclipse TE300 microscope (Nikon Corp., Tokyo, Japan) equipped with a 40× oil immersion objective (N.A. 1.3) and a Bio-Rad Radiance 2100MP confocal system (Zeiss/Bio-Rad, Hertfordshire, UK). Multichannel images were recorded by sequential excitation using 488-, 543-, and 637-nm lasers. Images were acquired using settings adjusted for submaximal confocal settings (at least 50% of extracellular pixel values below threshold value and 0.1–0.5% of pixel values inside the oocyte above maximal pixel value), and analysed using ImageJ (NIH; http://rsb.info.nih.gov/ij/). Submaximal confocal settings were also used to measure spindle recruitment since variations in spindle location and orientation cause large differences in diffraction due to the large size and high lipid content of oocytes (Supplementary Movie 5, see section on supplementary data given at the end of this article). Spindle recruitment was determined by dividing GFP fluorescence intensity on meiotic spindles by that in cortical regions as indicated. Images shown are maximum intensity Z projections of six consecutive confocal sections (unless otherwise indicated) taken at 2 μm intervals and subjected to limited contrast/brightness enhancements up to ∼20%. Control images were produced with the highest settings and enhancements used to create images of specific antibody stainings from the same experiment. Supplementary Movies were produced using ImageJ and the VolumeJ plugin (Abramoff & Viergever 2002) as described in the supplementary data.

Statistical analysis

Student's *t*-tests and χ^2 tests were performed in Microsoft Excel, and multinomial regression was performed in the R environment (www.r-project.org) using the 'lmer' function of the lme4 package (R package version 0.999375-28, http://lme4.r-forge.r-project.org). *P* values were considered significant at $P<0.05$ (Bonferroni corrected). Mean percentages and S.E.M. were weighted by the number of oocytes in each experiment.

Supplementary data

This is linked to the online version of the paper at http://dx.doi.org/10.1530/REP-10-0045.

Declaration of interest

The authors declare that there is no conflict of interest that could be perceived as prejudicing the impartiality of the research reported.

Funding

This research did not receive any specific grant from any funding agency in the public, commercial, or not-for-profit sector.

Acknowledgements

We thank the people at the Department of Farm Animal Health for their help with collecting oocytes, P J S van Kooten for production and isolation of CON.1 and X22 antibodies, A de Graaff and R Wubbolts at the Centre for Cellular Imaging for their technical assistance, L C Penning for his help with primer development, E M van t Veld for her practical contributions to this work and H Vernooij for statistical advice. We are grateful to A de Vreeden and D R Gutknecht at the University Medical Center for their assistance with and helpful comments on the microinjection procedure.

References

Abramoff MD & Viergever MA 2002 Computation and visualization of three-dimensional soft tissue motion in the orbit. *IEEE Transactions on Medical Imaging* **21** 296–304.

Acton SL & Brodsky FM 1990 Predominance of clathrin light chain LCb correlates with the presence of a regulated secretory pathway. *Journal of Cell Biology* **111** 1419–1426.

Albertson R, Riggs B & Sullivan W 2005 Membrane traffic: a driving force in cytokinesis. *Trends in Cell Biology* **15** 92–101.

Amano T, Mori T & Watanabe T 2004 Activation and development of porcine oocytes matured *in vitro* following injection of inositol 1,4,5-trisphosphate. *Animal Reproduction Science* **80** 101–112.

Bjerregaard B & Maddox-Hyttel P 2004 Regulation of ribosomal RNA gene expression in porcine oocytes. *Animal Reproduction Science* **82–83** 605–616.

Borlido J, Veltri G, Jackson AP & Mills IG 2008 Clathrin is spindle-associated but not essential for mitosis. *PLoS ONE* **3** e3115.

Bouniol-Baly C, Hamraoui L, Guibert J, Beaujean N, Szollosi MS & Debey P 1999 Differential transcriptional activity associated with chromatin configuration in fully grown mouse germinal vesicle oocytes. *Biology of Reproduction* **60** 580–587.

Brodsky FM 1985 Clathrin structure characterized with monoclonal antibodies. I. Analysis of multiple antigenic sites. *Journal of Cell Biology* **101** 2047–2054.

Cayrol C, Cougoule C & Wright M 2002 The beta2-adaptin clathrin adaptor interacts with the mitotic checkpoint kinase BubR1. *Biochemical and Biophysical Research Communications* **298** 720–730.

De La Fuente R & Eppig JJ 2001 Transcriptional activity of the mouse oocyte genome: companion granulosa cells modulate transcription and chromatin remodeling. *Developmental Biology* **229** 224–236.

DiLuigi A, Weitzman VN, Pace MC, Siano LJ, Maier D & Mehlmann LM 2008 Meiotic arrest in human oocytes is maintained by a Gs signaling pathway. *Biology of Reproduction* **78** 667–672.

El-Jouni W, Haun S, Hodeify R, Hosein WA & Machaca K 2007 Vesicular traffic at the cell membrane regulates oocyte meiotic arrest. *Development* **134** 3307–3315.

Fair T, Hyttel P, Greve T & Boland M 1996 Nucleus structure and transcriptional activity in relation to oocyte diameter in cattle. *Molecular Reproduction and Development* **43** 503–512.

Feng B, Schwarz H & Jesuthasan S 2002 Furrow-specific endocytosis during cytokinesis of zebrafish blastomeres. *Experimental Cell Research* **279** 14–20.

Goud B, Huet C & Louvard D 1985 Assembled and unassembled pools of clathrin: a quantitative study using an enzyme immunoassay. *Journal of Cell Biology* **100** 521–527.

Hinckley M, Vaccari S, Horner K, Chen R & Conti M 2005 The G-protein-coupled receptors GPR3 and GPR12 are involved in cAMP signaling and maintenance of meiotic arrest in rodent oocytes. *Developmental Biology* **287** 249–261.

Hölzenspies JJ, Stoorvogel W, Colenbrander B, Roelen BA, Gutknecht DR & van Haeften T 2009 CDC2/SPDY transiently associates with endoplasmic reticulum exit sites during oocyte maturation. *BMC Developmental Biology* **9** 8.

Jones KT 2008 Meiosis in oocytes: predisposition to aneuploidy and its increased incidence with age. *Human Reproduction Update* **14** 143–158.

Kirchhausen T 2000 Clathrin. *Annual Review of Biochemistry* **69** 699–727.

Lee GM 1989 Measurement of volume injected into individual cells by quantitative fluorescence microscopy. *Journal of Cell Science* **94** 443–447.

Lehtonen S, Shah M, Nielsen R, Iino N, Ryan JJ, Zhou H & Farquhar MG 2008 The endocytic adaptor protein ARH associates with motor and centrosomal proteins and is involved in centrosome assembly and cytokinesis. *Molecular and Cellular Biology* **19** 2949–2961.

Lince-Faria M, Maffini S, Orr B, Ding Y, Claudia F, Sunkel CE, Tavares A, Johansen J, Johansen KM & Maiato H 2009 Spatiotemporal control of mitosis by the conserved spindle matrix protein Megator. *Journal of Cell Biology* **184** 647–657.

Liu SH, Wong ML, Craik CS & Brodsky FM 1995 Regulation of clathrin assembly and trimerization defined using recombinant triskelion hubs. *Cell* **83** 257–267.

Liu SH, Marks MS & Brodsky FM 1998 A dominant-negative clathrin mutant differentially affects trafficking of molecules with distinct sorting motifs in the class II major histocompatibility complex (MHC) pathway. *Journal of Cell Biology* **140** 1023–1037.

Maro B, Johnson MH, Pickering SJ & Louvard D 1985 Changes in the distribution of membranous organelles during mouse early development. *Journal of Embryology and Experimental Morphology* **90** 287–309.

Martin RH 2008 Meiotic errors in human oogenesis and spermatogenesis. *Reproductive Biomedicine Online* **16** 523–531.

Mehlmann LM 2005*a* Oocyte-specific expression of Gpr3 is required for the maintenance of meiotic arrest in mouse oocytes. *Developmental Biology* **288** 397–404.

Mehlmann LM 2005*b* Stops and starts in mammalian oocytes: recent advances in understanding the regulation of meiotic arrest and oocyte maturation. *Reproduction* **130** 791–799.

Mehlmann LM, Saeki Y, Tanaka S, Brennan TJ, Evsikov AV, Pendola FL, Knowles BB, Eppig JJ & Jaffe LA 2004 The Gs-linked receptor GPR3 maintains meiotic arrest in mammalian oocytes. *Science* **306** 1947–1950.

Montagnac G & Chavrier P 2008 Endosome positioning during cytokinesis. *Biochemical Society Transactions* **36** 442–443.

Montagnac G, Echard A & Chavrier P 2008 Endocytic traffic in animal cell cytokinesis. *Current Opinion in Cell Biology* **20** 454–461.

Moore CA, Milano SK & Benovic JL 2007 Regulation of receptor trafficking by GRKs and arrestins. *Annual Review of Physiology* **69** 451–482.

Motlik J, Kopecny V, Travnik P & Pivko J 1984 RNA synthesis in pig follicular oocytes. Autoradiographic and cytochemical study. *Biology of the Cell* **50** 229–235.

Nathke IS, Heuser J, Lupas A, Stock J, Turck CW & Brodsky FM 1992 Folding and trimerization of clathrin subunits at the triskelion hub. *Cell* **68** 899–910.

Niswonger ML & O'Halloran TJ 1997 A novel role for clathrin in cytokinesis. *PNAS* **94** 8575–8578.

Ohashi S, Naito K, Liu J, Sheng Y, Yamanouchi K & Tojo H 2001 Expression of exogenous proteins in porcine maturing oocytes after mRNA injection: kinetic analysis and oocyte selection using EGFP mRNA. *Journal of Reproduction and Development* **47** 351–357.

Okamoto CT, McKinney J & Jeng YY 2000 Clathrin in mitotic spindles. *American Journal of Physiology. Cell Physiology* **279** C369–C374.

Richard FJ 2007 Regulation of meiotic maturation. *Journal of Animal Science* **85** E4–E6.

Royle SJ & Lagnado L 2006 Trimerisation is important for the function of clathrin at the mitotic spindle. *Journal of Cell Science* **119** 4071–4078.

Royle SJ, Bright NA & Lagnado L 2005 Clathrin is required for the function of the mitotic spindle. *Nature* **434** 1152–1157.

Schweitzer JK, Burke EE, Goodson HV & Souza-Schorey C 2005 Endocytosis resumes during late mitosis and is required for cytokinesis. *Journal of Biological Chemistry* **280** 41628–41635.

Ungewickell EJ & Hinrichsen L 2007 Endocytosis: clathrin-mediated membrane budding. *Current Opinion in Cell Biology* **19** 417–425.

Wang J & Liu XJ 2003 A G protein-coupled receptor kinase induces *Xenopus* oocyte maturation. *Journal of Biological Chemistry* **278** 15809–15814.

Warner AK, Keen JH & Wang YL 2006 Dynamics of membrane clathrin-coated structures during cytokinesis. *Traffic* **7** 205–215.

Wettey FR, Hawkins SF, Stewart A, Luzio JP, Howard JC & Jackson AP 2002 Controlled elimination of clathrin heavy-chain expression in DT40 lymphocytes. *Science* **297** 1521–1525.

Yamauchi T, Ishidao T, Nomura T, Shinagawa T, Tanaka Y, Yonemura S & Ishii S 2008 A B-Myb complex containing clathrin and filamin is required for mitotic spindle function. *EMBO Journal* **27** 1852–1862.

Received 25 January 2010
First decision 23 February 2010
Revised manuscript received 17 May 2010
Accepted 2 June 2010